

Article

Advanced Processes in Water Treatment: Synergistic Effects of Hydrodynamic Cavitation and Cold Plasma on Rhodamine B Dye Degradation

Federico Verdini ¹, Daniele Crudo ², Valentina Bosco ², Anna V. Kamler ³, Giancarlo Cravotto ^{1,*} and Emanuela Calcio Gaudino ^{1,*}

¹ Dipartimento di Scienza e Tecnologia del Farmaco, University of Turin, Via P. Giuria 9, 10125 Turin, Italy; federico.verdini@unito.it

² E-PIC S.r.l., Via XXIV Maggio 20, 13888 Mongrando, Italy; daniele.crudo@epic-srl.com (D.C.); valentina.bosco@epic-srl.com (V.B.)

³ Federal State Budgetary Institution of Science Kurnakov Institute of General and Inorganic Chemistry, Russian of Academy of Sciences, Leninskii Prosp. 31, 119071 Moscow, Russia; abramova@physics.msu.ru

* Correspondence: giancarlo.cravotto@unito.it (G.C.); emanuela.calcio@unito.it (E.C.G.); Tel.: +39-011-670-7183 (G.C.)

Abstract: The increasing pollution of water bodies, due to the constant release of highly toxic and non-biodegradable organic pollutants, requires innovative solutions for environmental remediation and wastewater treatment. In this study, the effectiveness of different Advanced Oxidation Processes (AOPs) for the purification of water contaminated with Rhodamine B (RhB) dye at a concentration of 5 mg/L were investigated and compared. Using the classical ozonation strategy as a benchmark treatment, the research showed over 99% degradation of RhB within 4 min in a laboratory-scale batch setup with a capacity of 0.2 L. In contrast, a “chemical-free” process exploiting ultrasound (US) technology achieved a 72% degradation rate within 60 min. Further experiments were conducted using a pilot-scale rotor-stator hydrodynamic cavitation (HC) reactor on a 15 L solution leading to 33% of RhB removal in the presence of hydrogen peroxide (H₂O₂) at 75 mg/L. However, the use of an innovative cavitation reactor, which hybridizes HC with cold plasma, showed remarkable efficiency and achieved 97% degradation of RhB in just 5 min when treating a 5 L solution at an inlet pressure of 20 bar in a loop configuration. In addition, a degradation rate of 58% was observed in a flow-through configuration, emphasising the robustness and scalability of the HC/electrical discharge (ED) plasma technology. These results underline the potential of hybrid HC/ED plasma technology as an intensified and scalable process for the purification of water, as it offers a catalyst- and oxidant-free protocol.

Keywords: hydrodynamic cavitation; ultrasound; cold plasma; electrical discharge; water purification; advanced oxidation processes; hybrid cavitation treatment; rhodamine B; sustainable water treatment



Citation: Verdini, F.; Crudo, D.; Bosco, V.; Kamler, A.V.; Cravotto, G.; Calcio Gaudino, E. Advanced Processes in Water Treatment: Synergistic Effects of Hydrodynamic Cavitation and Cold Plasma on Rhodamine B Dye Degradation. *Processes* **2024**, *12*, 2128. <https://doi.org/10.3390/pr12102128>

Academic Editors: Hayet Djelal and Andrea Petrella

Received: 4 August 2024

Revised: 26 September 2024

Accepted: 27 September 2024

Published: 30 September 2024



Copyright: © 2024 by the authors. Licensee MDPI, Basel, Switzerland. This article is an open access article distributed under the terms and conditions of the Creative Commons Attribution (CC BY) license (<https://creativecommons.org/licenses/by/4.0/>).

1. Introduction

The growing presence of contaminants of emerging concern (CECs) and dyes in various water sources represents a significant environmental issue, posing serious risks to both human health and aquatic ecosystems. According to the European Union [1], textile and dye industries are one of the main contributors (~20%) to global water pollution. The inefficient disposal or treatment of industrial textile wastewater, especially from dyeing and finishing processes, leads to a continuous release of hazardous heavy metals (e.g., metal complex acid dyes and metal-containing dyes) and harmful CECs such as dyes into lakes and rivers [2]. Due to their high chemical stability, rhodamine (Rh) compounds are the most frequently used dyes in textile industries. Due to its extensive use, global Rh production is projected to reach a value of \$232.5 million during the 2022–2027 forecast period [3].

Among the Rh dyes family, Rhodamine B (RhB) (Figure S1), also known as Basic Violet 10, is the most important xanthene dye used in textiles for dyeing cotton and leather, as well as being used in the paper, plastic, and cosmetics industries, as it is highly water soluble, non-volatile, and stable [4]. RhB is also extensively exploited in biological applications such as fluorescence imaging due to its remarkable photo-properties, including photostability and high brightness [5].

However, the discharge of RhB-polluted effluents into water bodies causes harmful effects on aquatic fauna such as tissue necrosis, respiratory and reproductive damages, or cancer [6]. In addition, when RhB enters the human body, it induces oxidative stress on cells and tissues, leading to irritation of the respiratory system, eyes, and skin, [7] as well as potential genetic mutations. [8]. Advanced oxidation processes (AOP) offer potential for the treatment of refractory dyes in wastewater; however, the development of efficient systems specifically for the degradation of dyes remains a major challenge [9].

Several physical processes such as membrane filtration [10], activated charcoal adsorption [11], and coagulation [12] are already used for the removal of dyes from industry effluents. Nevertheless, the above-mentioned technologies only transfer the pollutant from water to another solid or liquid waste (non-destructive) [13]. Therefore, the development of new technological, chemical-free processes for the degradation of RhB in industrial wastewater from the textile industry (end-of-pipe water treatment) is crucial. AOPs have emerged as promising technologies for the removal of dyes from contaminated water bodies by the generation of oxidizing radicals ($\cdot\text{OH}$, $\cdot\text{OOH}$, $\cdot\text{O}$, etc.) [14]. However, the most commonly studied AOPs such as Fenton, ozonation, or H_2O_2 require an extensive use of chemicals, strict operating conditions, and safety drawbacks. Therefore, in this study we compared conventional ozonation treatment with different scalable and “chemicals-free” cavitation AOPs such as ultrasound (US) and hydrodynamic cavitation (HC) at both laboratory and pilot scales and either alone or in the presence of external oxidizing compounds. Additionally, an innovative hybrid HC/ED plasma pilot-scale reactor was exploited for the sustainable intensification of RhB degradation processes. All the experiments were carried out dissolving RhB in tap water (composition reported in Table S1) to simulate a hypothetical treatment of dye-contaminated water.

2. Materials and Methods

2.1. Chemicals

All chemical have been provided by Merck-Sigma-Aldrich, Milan (Italy).

2.2. RhB Quantitative Analysis

The concentration of RhB in all the treated samples was spectrophotometrically measured using a UV-vis spectrophotometer (Agilent Cary 60 UV-vis) at 554 nm. The calibration curve (Figure S2) was calculated from standard RhB solutions (4, 3, 2, 1, 0.5, and 0.1 mg/mL) by proper dilutions in 2 mL volumetric flasks starting from a stock solution of 5 mg/mL. All the samples were prepared using tap water.

2.3. Lab-Scale O_3 -Assisted RhB Degradation

Preliminary RhB degradation experiments were carried out using O_3 as an oxidizing compound by using a 15 W O_3 generator (CQ-8025, Tianchang Changqing Mechanical and Electrical Trading Co., Ltd., Tianchang, China). For all the batch treatments, a porous ceramic septum connected to the O_3 generator was submerged in the RhB-contaminated solutions (Figure 1a) with a starting concentration of 5 mg/L (0.2 L and 0.5 L) into an Erlenmeyer flask. The input O_3 amount was 6.12 g/h at a flow rate of 6 L/h [15]. O_3 -treated samples were collected every 30 s or 1 min.

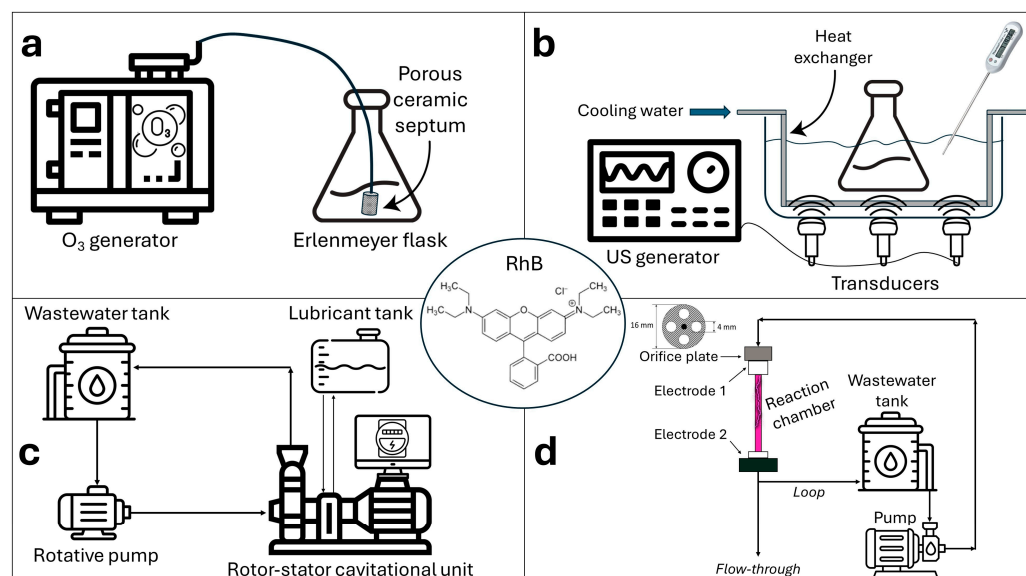


Figure 1. Schematics of each equipment used for the RhB degradation experiments. (a) lab-scale O₃, (b) lab-scale US, (c) rotor-stator HC, (d) hybrid HC/ED plasma.

2.4. Lab-Scale US-Assisted RhB Degradation

US-assisted RhB degradation treatments were carried out in a stainless-steel ultrasonic bath equipped with three piezo transducers. The output power of the US generator (Weber Ultrasonics AG, Karlsbad, Germany) was 200 W at a frequency of 500 kHz. All the experiments were carried out on 0.2 L RhB tap-water solutions (5 mg/L) placed in an Erlenmeyer 0.5 L flask submerged in the deionized water contained in the US bath (3 L), as shown in Figure 1b. The US density ratio was 62.5 W/L. The temperature was kept constant at 25 ± 2 °C by using a heat exchanger submerged in the US bath and connected to the tap-water line. Samples were collected every 5, 10, or 15 min of sonication time. The same protocol was used for the hybrid US/H₂O₂ treatments, carried out with 1:100 and 1:200 RhB:H₂O₂ mole ratios (H₂O₂ loadings of 37.5 and 75 mg/L, respectively).

2.5. Rotor-Stator HC-Assisted RhB Degradation at Pilot Scale

The HC-assisted pilot-scale RhB degradation tests were carried out in the commercially available ROTOCAP (E-PIC S.r.l., Italy) rotor-stator device connected to a 20 L stainless-steel reservoir tank and a rotative pump (Bronzoni Motori Elettrici Srl, Italy) for the recirculation of the contaminated solution (Figures 1c and S3). HC is generated by forcing contaminated water through its rotating cylinder equipped with a 4-kW electric engine. A chiller unit (DLSB-5/10, Zhengzhou Keda Machinery and Instrument Equipment Co., Ltd., Zhengzhou, Henan, China) set at -10 °C was linked to the heat exchanger placed inside the reservoir tank. Two different tests were performed in 15 L of a 5 mg/L RhB solution at a flow rate of 3000 L/h for a total time of 60 min (n° of passes = 200). The first experiment was carried out without the addition of an external oxidizing compound, while the second test was performed in the presence of H₂O₂ with a RhB:H₂O₂ molar ratio of 1:200. Treated samples were collected every 5, 10, or 15 min.

2.6. Hybrid HC/ED Plasma-Assisted Degradation of RhB

The hybrid pilot-scale HC/ED plasma reactor used for the degradation of RhB (Figures 1d and S4) was described in detail in a previous work [16]. Hydrodynamic cavitation was ensured using a 4-holed (4 mm for each hole) orifice plate and a 3.3 kW triplex plunger pump (SPECK Pumpen Verkaufsgesellschaft GmbH, Neunkirchen am Sand, Germany). The orifice plate is located at the top of a quartz cylinder discharge chamber characterized by a length of 200 mm and a diameter of 8 mm). The ED plasma was ignited by applying a 0.6 A alternating current (AC) with a voltage of 15 kV at a frequency of

48 kHz between two electrodes located at the ends of the quartz cylinder (distance of 200 mm).

In detail, the HC/ED plasma reactor uses the propagation of the electrical discharge in bubbles or vapor. No electrical discharge plasma can be generated without cavitation bubbles [16]. The degradation experiments were carried out in 5 L RhB solutions with a fixed starting concentration of 5 mg/L. Three sets of experiments were carried out at different inlet pressure values (10, 15 and 20 bar). The temperature of the treated water was kept constant at 27 ± 2 °C by using a chiller unit (DLSB-5/10, Zhengzhou Keda Machinery, and Instrument Equipment Co., Ltd., Zhengzhou, Henan, China) set at -10 °C and connected to the heat exchanger of a 30 L stainless-steel reservoir tank. Samples were collected either in flow-through configuration or after 1, 2, 5, and 10 min of recirculation time. Additional operating parameters are reported in the following table (Table 1).

Table 1. Main operating parameters of the HC/ED plasma degradation treatments.

Inlet Pressure (bar)	Flow Rate (L/h)	τ_R (min) ¹	t_R (min) ²	n° of Passes ²
10	250	0.0024	0.02	12.50
15	300	0.0020	0.02	15.00
20	330	0.0018	0.02	16.50

¹ Residence time for flow-through configuration; ² Residence time and number of passes for 10 min loop configuration.

3. Results

To better compare the efficiency of each considered AOP (O_3 -, US, and HC-assisted), a fixed RhB concentration of 5 mg/L was chosen, as this is the standard C0 in most reported studies [3]. Moreover, a tap-water solution was used as benchmark RhB to avoid the common practice of using distilled water for AOP research.

3.1. Lab-Scale O_3 -Assisted RhB Degradation

Due to (i) decreased costs associated with the production of O_3 , (ii) environmental advantages over chlorine-based degradation treatment, (iii) the possibility of treating wastewater contaminated by recalcitrant organic compounds such as dyes, and (iv) the reduction of sludges in WWTPs, the popularity of O_3 -based AOPs has grown in recent years [17,18].

The high oxidation potential of O_3 (2.08 V) makes the ozonation process very effective in the degradation of CECs and dyes such as RhB [19].

However, ozonation suffers from some drawbacks:

- Limited mass transfer in water because of O_3 low solubility and stability in water [20];
- Necessity for on-site production with typical low efficiencies (4–6 wt.% from air and 6–12 wt.% from pure oxygen) because of difficult storage and transportation [21];
- Low mineralization of pollutants [22].

During the O_3 -assisted degradation treatments, the organic pollutants can be directly oxidized by the O_3 molecule (direct method) or by the hydroxyl radicals generated after the decomposition of O_3 with contaminants (radical method) [23]. Generally, in acidic water solutions the direct method predominates while in alkaline environments the radical methods prevail [24]. In an intermediate pH range (6–8), both mechanisms can take place.

Aiming to preliminarily investigate the degradation of RhB at lab-scale, two ozonation treatments were performed on two different tap-water RhB solutions (0.2 L and 0.5 L) with the same starting concentration of contaminant (5 mg/L) and characterized by a pH value of 8. The O_3 was directly bubbled in the contaminated solutions at a fixed O_3 input rate (6.12 mg/h) and dosage rate (6 L/h). When treating the 0.2 L solution, quantitative RhB degradation (>99%) was achieved after only 4 min of treatment time, while at the end of the scale-up experiment, which was performed with a volume of 0.5 L, a maximum degradation rate of 92% was achieved (Final RhB concentration: 0.09 mg/L) (Figure 2).

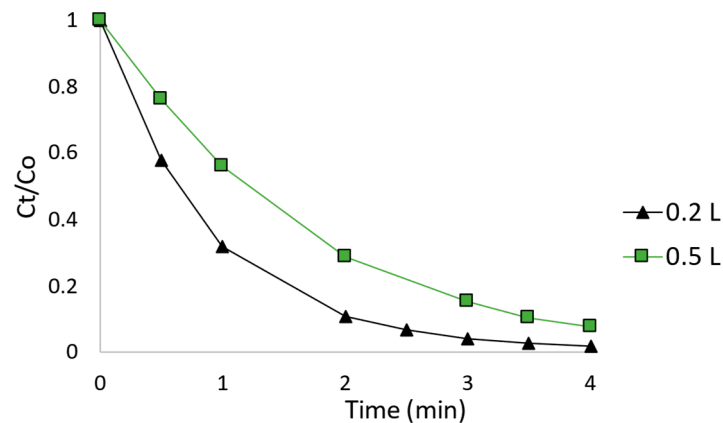


Figure 2. C_t/C_0 ratio of O_3 -assisted degradation treatments carried out on the 0.2 L (■) and the 0.5 L (▲) RhB solutions. Conditions: $C_{0\text{RhB}} = 5\text{ mg/L}$; $\text{pH} = 8$; O_3 input rate = 6.12 mg/h ; O_3 dosage = 6 L/h .

The kinetic evaluation of the previously described experiments highlighted the slow-down of the oxidation rate as a function of treated volume. The linearization of the pseudo-first order kinetic law (Equation (1)) revealed constant rate values of 1.0161 min^{-1} and 0.6447 min^{-1} for the degradation carried out on the 0.2 L and 0.5 L RhB solutions, respectively, as shown in Figure 3.

$$\frac{d[A]}{dt} = -k \cdot [A] \quad (1)$$

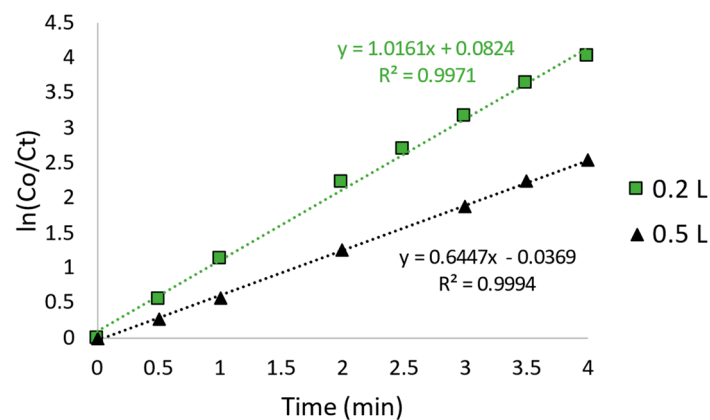


Figure 3. Kinetics of O_3 -assisted RhB degradation carried out on the 0.2 L (■) and the 0.5 L (▲) RhB solutions. Conditions: $C_{0\text{RhB}} = 5\text{ mg/L}$; $\text{pH} = 8$; O_3 input rate = 6.12 mg/h ; O_3 dosage = 6 L/h .

A fast O_3 -assisted RhB degradation was also achieved by Cuiping et al. [25] during the treatment carried out on a 100 mL RhB solution characterized by an initial concentration (C_0) of 100 mg/L . After prior optimization of the ozone dosage (1.8 L/h) at a fixed 5 g/h input rate, the authors achieved a dye degradation of 92.2% after 20 min in an acidic environment ($\text{pH} = 3$), with a consequent constant rate of 0.5214 min^{-1} . Additional tests were performed in a pH range of 4–10, but no noticeable effects on the extent of degradation rates were observed; even in alkaline conditions, the final degradation rates ($\sim 90\%$) were similar to that achieved at a pH of 3. A similar degradation test was carried out by Zawadzki et al. [26] for the degradation of RhB dissolved in 0.5 L of water ($C_0 = 20\text{ mg/L}$) at a corrected pH value of 6 with a fixed O_3 input rate and a dosage of 60 mg/h and 0.6 L/h , respectively. In such operative conditions, the authors observed a maximum RhB degradation of 75% after 30 min with a constant rate value of 0.0459 min^{-1} . To increase the dye degradation, the same authors performed a hybrid O_3/UV aiming to accelerate the O_3 decomposition and

intensify the hydroxyl radical ($\cdot\text{OH}$) production. The coupling of UV to O_3 successfully allowed it to increase the RhB degradation from 75% to 90% and the constant rate from 0.0459 to 0.0726 min^{-1} .

In general, our RhB preliminary degradation tests, together with the results published in the literature, have shown that ozone is an excellent and efficient oxidizing agent for the purification of RhB-contaminated water sources. However, for the treatment of large volumes and high RhB concentrations, ozonation alone may be less efficient, and its hybridization with other AOPs should be considered for the intensification of degradation processes to promote an efficient scaling up at industrial levels. In addition, O_3 -based plants for water treatment require complex equipment and control systems (mainly due to the corrosiveness of O_3) resulting in high operating and maintenance costs [27].

3.2. Lab-Scale US-Assisted RhB Degradation

Recently, cavitation technologies such as US (acoustic cavitation) emerged as effective candidates for the sustainable purification of both industrial effluents and naturally polluted water sources [28]. In contrast to conventional AOPs such as Fenton, ozonation, and photoelectro- and UV-catalysis (which require large amounts of chemicals), cavitation treatments are generally considered “green” processes for industrial-scale applications [29,30]. With respect to acoustic cavitation, the propagation of US waves (acoustic waves in the 20–800 kHz range) in water through compression and rarefaction cycles allows the generation of mainly $\cdot\text{OH}$, which can attack and degrade organic contaminants. In detail, when the negative pressure reached during the rarefaction cycle locally falls below the vapor pressure of water, vapor and dissolved gas cavities (i.e., cavitation bubbles) are formed. In the following compression cycle, the cavitation bubbles continue to grow, producing larger acoustic cavities. When the critical cavities reach an unstable size, they implode violently and generate high-pressure (>1000 bar) and high-temperature (thousand Kelvins) areas (i.e., hot spots) and shock waves. As a consequence, highly reactive free radicals are formed [31,32]. By varying the frequency of US waves, both physical and chemical effects can be produced. Generally, at low frequencies (20–100 kHz range), physical effects (e.g., increased turbulence in water) are predominant, while at higher frequencies (200–500 kHz range), the chemical effects (highly reactive radicals production) dominate because of the generation of a large number of cavities [33] characterized by a shorter lifetime, which enables more $\cdot\text{OH}$ migration from the cavities and results in a higher proportion of radical reactions in the bulk solution [34,35]. For this reason, in this work, different RhB degradation experiments were performed under the effect of US at a frequency of 500 kHz with a power of 200 W. An initial US-only test was carried out on a 0.2 L RhB tap-water solution with a fixed initial RhB concentration of 5 mg/L (pH = 8) for a total treatment time of 60 min. To promote cavitation effects only (and avoid possible thermal degradation effects), a heat exchanger was used to keep the temperature of the water contained in the US-bath at a constant value of 25 ± 2 °C. As shown in Figure 4, 60 min of US alone allowed a RhB degradation of 72%. The constant rate of the degradation treatment was calculated by the linearization of the pseudo first-order kinetic law (Equation (1)), and it was 0.0216 min^{-1} (Figure S5). During the treatment, the power consumption was measured and was 0.150 kWh. Due to the prolonged treatment time required by US alone, two additional US-assisted degradation tests were conducted with H_2O_2 as an external oxidizing agent, supplementing the hydroxyl radicals ($\cdot\text{OH}$) generated by US. In fact, under hybrid US/ H_2O_2 treatments, US irradiation can dissociate H_2O_2 molecules into two $\cdot\text{OH}$ molecules, increasing their concentration into the contaminated water. In addition, undissociated H_2O_2 can act as a secondary source of oxidizing compounds [36]. Therefore, two hybrid US/ H_2O_2 treatments were carried out with two different RhB: H_2O_2 ratios (1:100 and 1:200) under the US-only operative conditions (0.2 L RhB tap-water solution with a fixed initial RhB concentration of 5 mg/L at a pH of 8). The addition of the external oxidizing compound generally led to an increase of the degradation rate achieved under US alone (72%). In detail, after 60 min of US/ H_2O_2 treatment performed with RhB: H_2O_2

ratios of 1:100 and 1:200, the achieved degradation rates were 82% and 90%, respectively, with an increase of constant rates up to 0.0283 min^{-1} and 0.0364 min^{-1} (Figures 4 and S4). The detailed degradation rate values as functions of all treatment times are reported in Appendix A (Table A1).

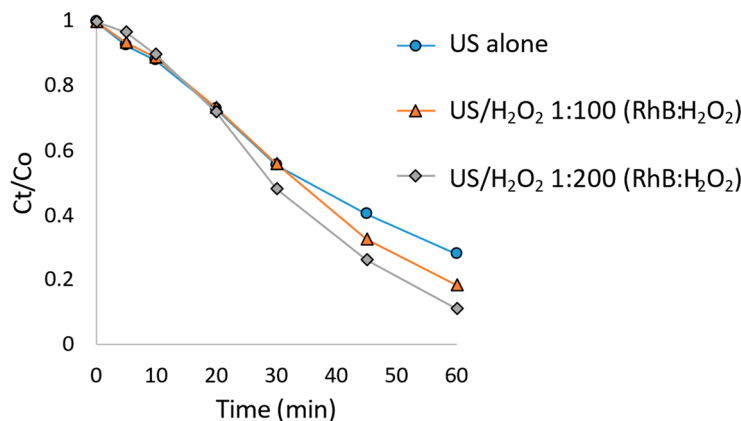


Figure 4. C_t/C_0 ratio of US-assisted degradation treatments carried out alone (●) or in presence of H_2O_2 with a RhB: H_2O_2 ratio of 1:100 (▲) and 1:200 (◆). Conditions: $C_{0 \text{ RhB}} = 5 \text{ mg/L}$; $\text{pH} = 8$; $V = 0.2 \text{ L}$.

The prolonged treatment time required for the RhB degradation under 500 kHz US can be ascribed to the low turbulence of treated solutions observed due the high-frequency US exploited (prevalent chemical effects). Despite the $\cdot\text{OH}$ oxidation potential (2.80 V) being higher than that of O_3 (2.01 V), both the higher oxidant quantity and the extreme turbulence (Figure S6) achieved during the O_3 -assisted degradation tests described in Section 3.1 allowed for a faster RhB degradation than that of US alone and US/ H_2O_2 (Table 2). In addition, the comparison of the O_3 -assisted (Figure 3) and US-assisted degradation dimensionless profiles (C_t/C_0) highlights two possible different degradation mechanisms. As described in Section 3.1, during O_3 -assisted degradation treatments the combination of direct and radical degradation mechanisms can take place, while under US the radical mechanism is predominant.

Table 2. Main operating parameters of the HC/ED plasma degradation treatments.

AOP Technology	RhB: H_2O_2	Volume Treated (L)	$k \text{ (min}^{-1}\text{)}$	Degradation Rate (%)
O_3	-	0.2	1.0161	>99
O_3	-	0.5	0.6447	92
US alone	-	0.2	0.0216	72
US/ H_2O_2	1:100	0.2	0.0283	82
US/ H_2O_2	1:200	0.2	0.0364	90

An increase in mass transfer under the 500 kHz US-assisted treatment could be achieved operating in a loop system with the recirculation of the contaminated solution. Unfortunately, the design of the US system used in this work cannot be adapted to perform experiments in loop configurations. So, to achieve a compromise between US physical and chemical effects, an additional test was carried out reducing the US frequency to 120 kHz at a fixed power of 200 W under the same operative conditions of the previous US-assisted experiments. However, even after 60 min of treatments, no RhB degradation was achieved. Despite US-based cavitation technologies having already been scaled up to pilot-scale levels for the efficient pretreatment of waste biomasses [37]; the highest US frequency generally deployed into such systems is 120 kHz, which did not allow the degradation of RhB in this work.

For the sake of comparison, several authors performed US-assisted RhB degradation treatments exploiting similar lab-scale US systems. Xu et al. [38] carried out several RhB degradation tests investigating the effect of the US power at a fixed frequency of 35 kHz in a US bath, using a stirrer to enhance the mass transfer. The combination of US and stirring allowed the authors to achieve a maximum RhB degradation rate of 86% after 40 min of sonication at 300 W on a 250 mL RhB solution characterized by an initial concentration of 20 mg/L. In addition to US bath systems, similar cavitation effects can be achieved by using a US probe (horn) dipped directly into the contaminated solution as carried out by Ye et al. [39]. The authors treated a 250 mL RhB solution ($C_0 = 10$ mg/L), dipping the US probe to a depth of 3 cm linked to a US generator set at a frequency of 20 kHz and at a power of 800 W. After the correction of the RhB solution pH at a value of 3, and at the end of the sonication treatment carried out for 100 min, the authors achieved a maximum degradation rate of 42%. With respect to US/H₂O₂ technologies, Mehrdad et al. [40] confirmed the benefits of such hybrid approaches (i.e., acceleration of degradation rate), increasing the constant rate observed under the effect of H₂O₂ alone from $1.73 \pm 0.02 \times 10^{-4}$ up to $7.64 \pm 0.02 \times 10^{-3} \text{ min}^{-1}$, and exploiting the hybrid US/H₂O₂ approach during the degradation of a 200 mL RhB solution ($C_0 = 60$ mg/L) using a US probe working at a frequency of 24 kHz. The presented results partially demonstrated the possibility of RhB dye degradation avoiding the use of oxidizing chemical compounds; however, to increase both the degradation and constant rates of US alone-assisted efficiencies, an external oxidizing compound should be added anyway with a limitation of the sustainability of the US treatments. In addition, the scalability at both pilot and industrial scales of US systems, designed specifically for the degradation of organic contaminants (i.e., high frequency, power, and mass transfer), still represents a challenge in recent years due to their typical low energy transfer efficiencies (10–40%) and a rapid decrease of cavitation intensity with distance from the ultrasonic transducer [41]. Limitations of US cavitation technologies from a scalability point of view will be challenged and described in the next section. Herein, it is important to point out that cavitation can also be generated in the hydraulic systems through which water flows (hydrodynamic cavitation; HC). In the case of HC, another physical AOP, pressure variations in the flowing liquid are generated by the passage of the fluid through constrictions such as orifice plates (single or multiple holes), Venturi tubes, or throttling valves [42]. In detail, HC takes place when the local pressure drops (according to Bernoulli's principle) below its corresponding vapor pressure at the constriction, with resulting formation of water vapor cavities (i.e., cavitation bubbles).

3.3. Rotor-Stator HC-Assisted RhB Degradation at Pilot Scale

As with US-generated cavities, because of the energy released during the implosion of HC cavities at the end of their lifecycle, mainly $\cdot\text{OH}$ and $\cdot\text{H}$ are generated by homolytic splitting of water molecule chemical bonds [43]. The same water pressure drop can be achieved in rotor-stator cavitation reactors between a spinning rotor and a fixed stator, as shown in Figure 5.



Figure 5. Generic structure of a rotor-stator cavitation reactor.

In detail, the fluid is propelled by the rotor and its direction matches to the rotational direction. The flow punches the back edge of the gap and forms a separation region with low pressure, and the cavities are formed when the rotational speed reaches the critical value [44]. Considering that HC systems are less expensive and more efficient in terms of energy transfer than US (specifically at pilot and industrial scale) [45], they have been widely used for wastewater purification in recent years [46]. For this reason, two different RhB degradation tests were carried out in the commercially available ROTOCARV (E-PIC S.r.l) rotor-stator HC reactor to investigate the possible scalability of HC-assisted water treatment at pilot scale. The first degradation treatment was performed by exploiting HC only cavitation effect on a 15 L RhB solution with an initial concentration of 5 mg/L. After 60 min of HC alone degradation treatment in recirculation approach (n° of passes = 200), the highest RhB degradation achieved was only 13% and the calculated constant rate value was 0.0024 min^{-1} as shown in Figure 6. The low degradation observed during the described treatment shows the limits of HC alone technology in the field of wastewater treatment. In fact, the efficiency of rotating HC reactors in treating water is strongly affected by several geometric and operative parameters [46] such as the following:

- Gap between the stator and the rotor;
- Diameter and geometry of both the rotor and stator;
- Presence of dimples, indentations, or vanes on rotor;
- Rotational speed;
- Power of electric motor.

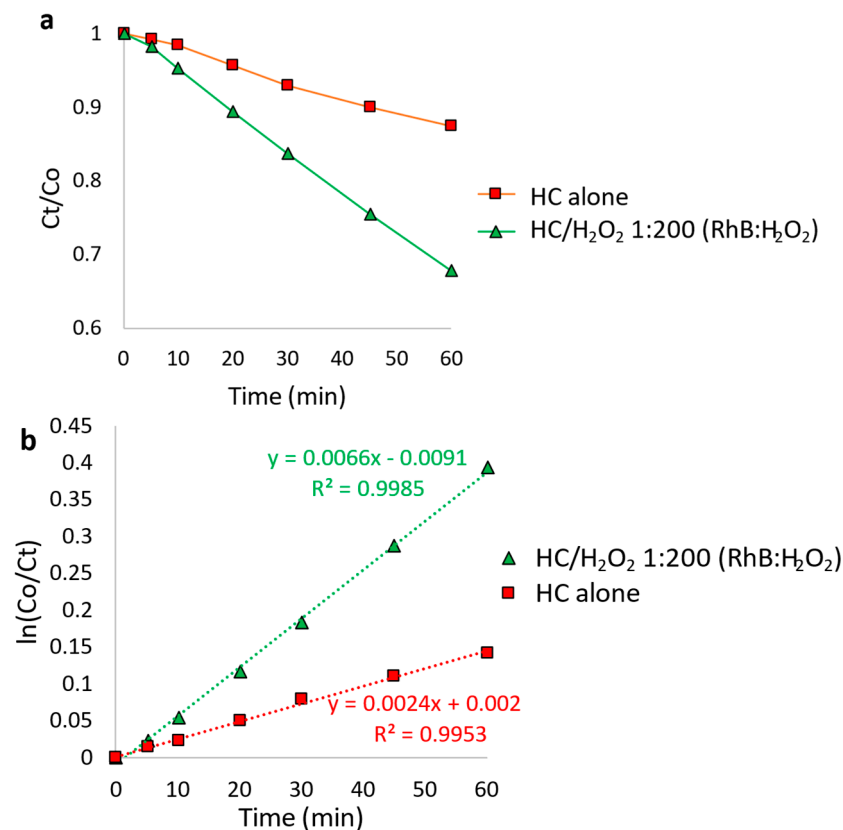


Figure 6. (a) C_t/C_0 ratio of HC-assisted degradation treatments carried out alone (■) or in presence of H_2O_2 with a RhB: H_2O_2 ratio of 1:200 (▲); (b) First-order linearization of HC-assisted experimental data. Conditions: $C_{0 \text{ RhB}} = 5 \text{ mg/L}$; $\text{pH} = 8$; $V = 15 \text{ L}$.

Due to the generally low pollutant degradation under HC treatment alone, a new trend in cavitation-based treatments in recent years has been the integration or hybridization of the treatment with other advanced oxidation processes (AOPs) or their combined use

with chemical oxidizing agents [47]. Based on the efficient combination of US and H₂O₂ with a RhB:H₂O₂ mole ratio of 1:200 observed in Section 3.2, and especially to avoid the production of large volumes of wastewater, the same operative conditions (RhB:H₂O₂ 1:200) were directly transposed on the pilot-scale HC system. The hybridization of HC and H₂O₂ allowed for increases in both the HC-only RhB degradation (13%) and the constant rate (0.0024 min⁻¹) up to 33% and 0.0066 min⁻¹, respectively (Figure 6). The detailed degradation rate values as functions of all treatment times are reported in Appendix A (Table A2).

For both HC alone and HC/H₂O₂ the total normalized energy consumption (HC system + pump + chiller unit) during the treatment was 1.38 kWh/m³ (3.85 kWh). Considering an average cost of 0.062 €/kWh for electricity supply in Italy [48], the cost of rotor-stator HC-assisted treatment alone is around 0.09 €/m³. In addition, the energy efficiency calculated for 60 min of treatment (according to Equation (2)) of HC alone was 2.39 mg/kWh, while for the HC/H₂O₂ it was 4.65 mg/kWh.

$$\text{Energy efficiency} = \frac{\text{mg of degraded RhB}}{\text{kWh}} \quad (2)$$

Although the HC system used can treat larger volumes than the previously used US unit, it showed a lower efficiency in the degradation of RhB dye. In detail, the geometry of the rotor-stator system deployed in this work was designed specifically for the pre-treatment of biomasses for methane production, for the extraction of food supplements and as a homogenizer for foodstuffs [49], and to produce biodiesel [50], and it was tested for water purification for the first time. However, for sake of comparison, Mishra et al. [51] tested an HC system equipped with a circular venturi constriction to treat a 4 L RhB solution with an initial dye concentration of 10 mg/L and a pH of 2.5, working with an inlet pressure of 4.9 bar at a fixed temperature of 40 °C. Under such operative conditions, the authors achieved a maximum RhB degradation of 65% after 120 min. To enhance the efficiency of the HC reactor, the authors subsequently performed a hybrid HC/Fenton (FeSO₄:H₂O₂ in the ratio of 1:5) degradation test under the same operative conditions, achieving a complete dye degradation after 120 min. An innovative swirling-jet cavitation system was exploited under both HC alone and hybrid HC/H₂O₂ (with a H₂O₂ loading of 100 mg/L) by Wang et al. [52] for treating a 25 L RhB solution with 10 mg/L initial concentration. Both treatments were carried out working with an inlet pressure of 60 bar. Under acidic conditions (pH = 3), the HC alone test allowed the authors to achieve an RhB degradation of about 65% after 180 min, while the HC/H₂O₂ guaranteed 99% dye removal. However, an increase in the starting pH of treated solutions to 7 and 10 decreased the degradation to about 75% and 64%, respectively, reflecting the efficiency decrease of the majority of AOPs carried out on RhB [3]. The presented experimental data, together with the literature, demonstrated the possibility of degradation of RhB by means of HC treatments; however, to increase their degradation efficiency (or to reduce the HC treatment time), an external oxidizing agent should be added. From a research point of view, the RhB degradation by means of AOPs is generally enhanced by an acidic pH of dye-contaminated solutions. Nevertheless, to effectively implement HC reactors to existing water treatment facilities, the correction of the starting pH could represent a bottleneck.

3.4. Pilot-Scale HC/ED-Assisted RhB Degradation

In very recent years, cold (or non-thermal) plasma technology has been recognized as a promising AOP for both soil and water remediation due to (i) its high efficiency in the degradation of CECs and recalcitrant water pollutants, (ii) minimal secondary pollution, (iii) relative low energy consumption, and (iv) short treatment times required [53]. In general, cold plasma can be generated by applying an electrical discharge (ED) to gases such as Ar, N₂, O₂, air, or even water vapor, with a consequent production of highly reactive species such as radicals ([•]OH, [•]O, or H), electrons, O₃, and ions by means of

electrons impacted with gas/vapor molecules (impact ionization mechanism), as simplified by Equations (3)–(7) [54].



Generally, ED-based plasma systems are composed of two electrodes connected to a power source and a working gas. In such systems, three different reactor designs can be exploited for the generation of highly reactive radicals responsible for the pollutant's degradation: a discharge in (i) gas phase, (ii) liquid phase, or (iii) hybrid gas–liquid phase [55,56]. In the gas phase geometry, ED plasma is generated in gas injected above the polluted water surface, while in the liquid phase approach, ED plasma is directly generated within the water. However, such ED reactors are characterized by low mass transfer of generated radicals, limiting the degradation rate of contaminants. To increase the migration of radicals towards the bulk water, ED plasma can be generated and propagated in the gas directly injected in the contaminated water solution or in water vapor bubbles (hybrid gas–liquid phase) [57]. Therefore, in the present work, a new and innovative hybrid ED plasma-based technology was exploited to generate ED plasma in the hybrid gas–liquid phase by coupling HC with ED cold plasma for the intensification of the water-remediation process. As demonstrated by Abramov et al. [58], ED can be efficiently propagated between the HC cavities to allow the generation of plasma both in their gas/vapor phase and at their gas–bulk liquid interface with consequent generation of oxidizing ($\cdot OH$, $\cdot O$, and O_3) and reducing species ($\cdot H$), thereby increasing the overall mass and energy transfer. In this work, a similar hybrid HC/ED plasma reactor (described in Section 2.5 and schematically illustrated in Figure 7) was exploited for the degradation of RhB due to the interesting and promising results achieved in previous works in which several CECs such as tetracyclines (TC) [16], metronidazole (MNZ) [59], furosemide (FUR) [60], and APIs contained in a real industrial effluent [61] were efficiently degraded in short treatment times without the need of external oxidizing compounds.

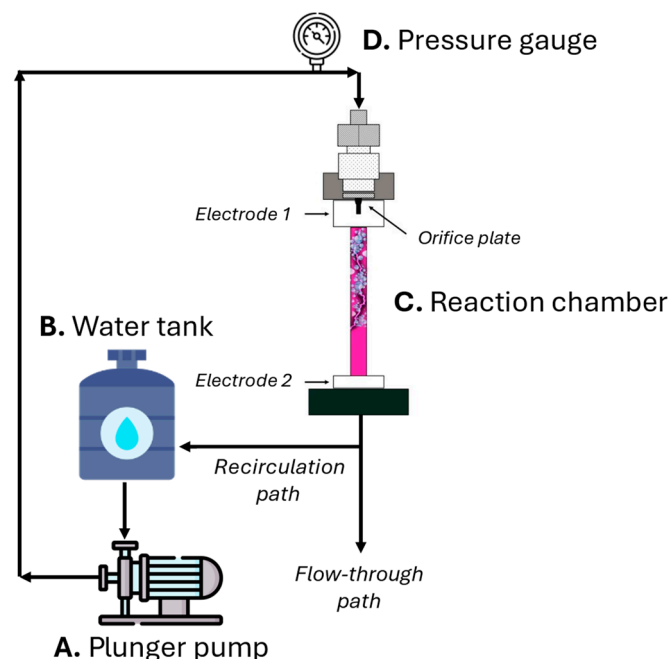


Figure 7. Schematic of the HC/ED plasma reactor used in this work.

Specifically, the plasma-assisted HC/ED degradation tests were all carried out using a 5 L RhB solution ($C_0 = 5$ mg/L), investigating the effect of the inlet pressure (10, 15, and 20 bar) and collecting samples either in flow-through or loop configurations. For comparison, an additional test was carried out under the effect of HC alone. As shown in Table 3, both HC alone and hybrid HC/ED plasma approaches achieved interesting results in flow-through with the highest degradation of 58% working with an inlet pressure of 20 bar under hybrid HC/ED plasma. As expected, the dye degradation decreased as the operating pressure was reduced to 15 bar (52%) and 10 bar (39%).

Table 3. Results of degradation tests performed in flow-through under both HC alone and hybrid HC/ED plasma.

Technology	Inlet Pressure (bar)	Flow Rate (L/h)	τ_R (min)	Degradation Rate in Flow-Through (%)
Hybrid HC/ED	10	250	0.0024	39
Hybrid HC/ED	15	300	0.0020	52
Hybrid HC/ED	20	330	0.0018	58
HC alone	20	330	0.0018	28

The lowest degradation was observed under HC alone (28%), demonstrating the effective synergism of HC and ED plasma during the hybrid experiments. However, the degradation achieved under HC alone (28%) was comparable to those achieved after 20 min of US alone, US/H₂O₂ 1:100 (27%), US/ H₂O₂ 1:200 (28%), and 45 min of rotor-stator HC/H₂O₂ (25%), revealing the higher efficiency of the hybrid reactor (in flow-through) even under the non-hybrid approach.

Substantial increases in RhB degradation were observed during the treatments carried out in loop configuration. As shown by the dimensionless profiles (C_t/C_0) reported in Figure 8, a quantitative dye degradation (97%) was achieved under hybrid HC/ED plasma after only 5 min of treatment carried out at 20 bar (Figure 9). To reach a similar degradation value (98%), the experiment performed at 15 bar required 10 min of treatment while a further decrease of inlet pressure (to 10 bar) allowed it to achieve a maximum degradation of 94% after 10 min. The detailed degradation rate values as functions of all treatment times are reported in Appendix A (Table A3).

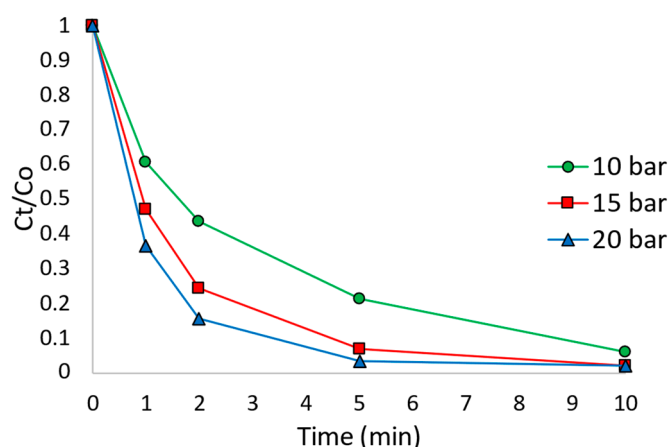


Figure 8. C_t/C_0 ratio of HC/ED-assisted degradation treatments carried out at 10 bar (●), 15 bar (■), and 20 bar (▲). Conditions: C_0 RhB = 5 mg/L; pH = 8; V = 5 L.

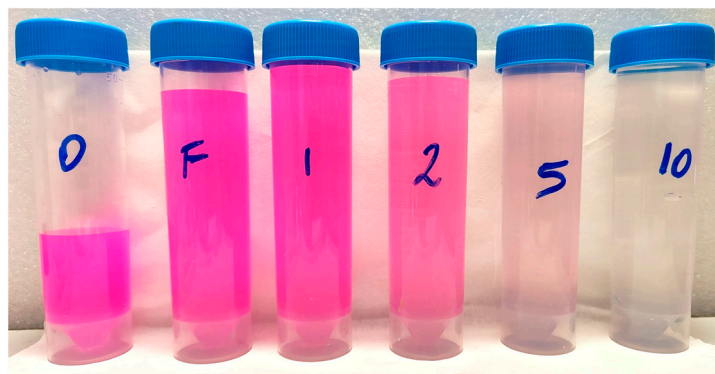


Figure 9. Picture of RhB solutions sampled during the HC/ED plasma treatment performed with an inlet pressure of 20 bar. 0: starting solution, F: flow-through treatment, 1: 1 min loop treatment, 2: 2 min loop treatment, 5: 5 min loop treatment, 10: 10 min loop treatment.

During the non-hybrid loop treatment (HC alone), the degradation did not increase (Figure S7) compared to that observed under flow conditions (27%), reflecting the same results achieved in the previous works [16,59] in which the sonochemical dosimetry revealed the formation of a constant concentration of oxidizing compounds under such operative conditions. In addition to an increase of the degradation rate, the rise in inlet pressure during HC/ED plasma experiments also resulted in an increase of the constant rates as reported in Table 4, achieving the highest constant rate of 0.6598 min^{-1} working at 20 bar. The linearization of experimental data, according to the pseudo-first order law (Equation (1)) and the UV-vis spectra are reported in Figures S8 and S9.

Table 4. Constant rate values of degradation tests performed at 10,15, and 20 bar in loop configuration under hybrid HC/ED plasma.

Inlet Pressure (bar)	k (min^{-1})	R ²
10	0.2983	0.9712
15	0.5256	0.9807
20	0.6598	0.9730

Furthermore, the normalized energy consumption (kWh/m^3) and the 10-min treatment energy efficiencies (mg/kWh) of each HC/ED plasma-assisted test were calculated and reported in Table 5. Although the best results in terms of degradation and constant rates were achieved operating with an inlet pressure of 20 bar, under such operative conditions the HC/ED plasma reactor revealed the highest normalized energy consumption (8.79 kWh/m^3) and consequent lowest energy efficiency (9.94 mg/kWh). In fact, from an energy consumption point of view, the best results were achieved at 10 bar, with a normalized energy consumption of 7.14 kWh/m^3 and an energy efficiency of 13.82 mg/kWh . Despite the energy consumptions (7.14 , 7.33 , and 8.79 kWh/m^3 at 10, 15, and 20 bar, respectively) and treatments costs (0.44 , 0.45 , and 0.55 €/m^3 at 10, 15, and 20 bar, respectively) of the hybrid HC/ED plasma reactor were greater than that of the rotor-stator HC system described in Section 3.3 (1.38 kWh/m^3 and 0.09 €/m^3), the energy efficiencies of the 10-min HC/ED plasma treatments (13.82 , 13.11 , and 9.94 mg/kWh at 10, 15, and 20 bar, respectively) were conspicuously higher than those of the 60-min rotor-stator HC alone and the rotor-stator HC/ H_2O_2 experiments (2.39 and 4.65 mg/kWh , respectively).

Table 5. Energy consumption and energy efficiency of HC/ED plasma-assisted RhB degradation experiments.

Inlet Pressure (bar)	Energy Consumption (kWh)	Normalized Energy Consumption (kWh/m ³)	Treatment Cost (€/m ³)	Energy Efficiency (mg/kWh) ¹
10	2.0	7.14	0.44	13.82
15	2.2	7.33	0.45	13.11
20	2.9	8.79	0.55	9.94

¹ Calculated for 10 min of treatment.

For comparison, a similar combined (and not hybrid) HC + plasma reactor (sequential plasma generation and subsequent HC) allowed Nie et al. [62] to achieve a maximum RhB degradation rate of 97% treating a 5 L solution ($C_0 = 5$ mg/L) at a pH of 3, with an inlet pressure of 20 bar after 120 min of treatment assisted by the injection of O₂ at a flow rate of 50 mL/min for the plasma ignition. According to the authors, the overall energy consumption of the treatment was 234.6 kW/m³. In recent years, US cavitation treatments have also been coupled with cold plasma for the degradation of RhB. Komarov et al. [63] reported a hybrid recirculating reactor composed of a US probe (horn) placed above a needle-shaped high-voltage electrode for degradation treatments to allow the propagation of pulsed ED between the generated cavities. The authors treated a 2.5 L solution of RhB with an initial concentration of 10 mg/L, and under the optimized operative condition (pH = 5; US power = 210 W; ED voltage = 25 kV; Flow rate = 60 L/h) achieved a 26% RhB degradation in 12 min of treatment. The same US/ED plasma system was used in a batch configuration by Xu et al. [64] in the presence of ferrous chloride (FeCl₂) and injected argon (8 L/min) for the US/ED plasma/Fenton-assisted degradation of the same dye. Working under a US frequency of 20 kHz at a power of 120 W, an ED voltage of 40 kV, and a FeCl₂ loading of 5 mg/L, the authors treated a 2 L RhB solution ($C_0 = 5$ mg/L) at a pH of 4, achieving a degradation efficiency of 77% in 12 min.

Regarding the presented results of the HC/ED plasma-assisted treatments, this technology has been shown to be more efficient than O₃ (given the 10-fold higher volume treated), US, and rotor-stator HC. It demonstrates superior performance in handling larger volumes, requires shorter treatment times, improves energy efficiency, and intensifies the process, all while eliminating the need for external oxidizing agents and gas injections for plasma ignition.

3.5. RhB Degradation: PROS and CONS of Screened AOPs

To better compare the effectiveness of the four degradative approaches studied in this article for rhodamine B, the PROS and CONS of each technological approach have been highlighted in Table 6. Although the HC/ED approach was found to be the best performer, detailed investigations about degradation mechanism and by-product formation are still required in the near future, as well as further investigation of potential HC/ED plasma industrial-scale use on more severe pollutant concentrations.

Table 6. PROS and CONS of screened AOPs for RhB degradation.

Technology	Pros	Cons
Lab-scale O ₃	<ul style="list-style-type: none"> - Fast degradation kinetics - Organic pollutant mineralization - No sludge production - Some plants already scaled-up at industrial level - High mass transfer - Possible simultaneous sterilization 	<ul style="list-style-type: none"> - Batch treatments - High capital and operating maintenance costs at industrial level - Low plant and worker safety - Low O₃ solubility in water - Energy cost - Possible formation of hazardous by-products - In site O₃ production required

Table 6. Cont.

Technology	Pros	Cons
Lab-scale US	<ul style="list-style-type: none"> - Lower energy consumption than rotor-stator HC and hybrid HC/ED plasma - Simple system design - Safe for workers - Easy operations 	<ul style="list-style-type: none"> - Low mass transfer (due to the high US frequencies required) - Batch treatments - Low degradation kinetics - Low scalability at industrial level for wastewater treatment - External chemicals required for mineralization of organic pollutants (combined/hybrid process) - Low energy efficiency
Rotor-stator HC	<ul style="list-style-type: none"> - Pilot scale - Moderately low treatment cost - Easily scalable at industrial level - Simple system design - Flow or loop treatments - Safe for workers - Easy operations - Pilot scale - Fast degradation kinetics - High energy efficiency - High efficiency already in flow-through - No sludge production - No external chemicals required 	<ul style="list-style-type: none"> - Low degradation kinetics - Detailed studies are still required to develop high-efficient rotor-stator devices for wastewater treatment - External chemicals are required to enhance HC treatments
Hybrid HC/ED plasma	<ul style="list-style-type: none"> - In-situ formation of different oxidizing chemicals [16] - pH independence [16] - Possible ED-induced pyrolysis of pollutants - Simple design - Easy operation - Higher efficiency than existing cold-plasma only technologies 	<ul style="list-style-type: none"> - Moderate-high treatment cost - Detailed investigations about degradation mechanism and by-product formation are still required - Possible prior removal of suspended solids required (due to the orifice plate restrictions) - Maintenance of electrodes and hydraulic section (due to working under pressure rather than suction)

4. Conclusions

In this study, different AOP technologies were compared with the aim of developing a sustainable and chemical-free wastewater treatment process for the purification of tap water ad-hoc contaminated by the RhB dye. The benchmark O₃-based treatment revealed a robust efficiency in the quantitative RhB degradation (>99%) after only 4 min of treatment time carried out at laboratory scale (0.2 L) in batch configuration.

In the US-assisted experiments, a maximum dye degradation of 72% was achieved after an extended treatment time of 60 min under the effect of US alone. However, relatively high hydrogen peroxide (H₂O₂) loadings of 37.5 and 75 mg/L were required to increase RhB degradation to 82% and 90%, respectively. Due to the limited scalability of the US process, an easily industrially scalable rotor-stator hydrodynamic cavitation (HC) unit was tested on larger volumes (15 L) of contaminated solutions in a loop configuration (recirculation). Nevertheless, because of the specific geometry of the rotor-stator system (primarily designed for biomass pretreatment), only 33% RhB degradation was achieved in the presence of H₂O₂ (75 mg/L) after 60 min.

In contrast, the hybrid HC/ED plasma technology achieved very rapid (5 min), nearly complete (97%), chemical-free, and energy-efficient RhB degradation in a 5 L solution at an inlet pressure of 20 bar in a loop configuration. It is noteworthy that significant RhB degradation rates (>39%) were also observed in a flow-through configuration.

In summary, the HC/ED plasma-assisted degradation experiments demonstrated the effective combination of hydrodynamic cavitation with cold plasma, which offers scalability and intensification of existing cavitation technologies for the purification of wastewater. The comparative analysis of various AOPs for treating water contaminated with simulated

RhB dye has offered valuable insights into their efficiency and scalability, particularly in terms of expanding cavitation processes to an industrial level.

Supplementary Materials: The following supporting information can be downloaded at: <https://www.mdpi.com/article/10.3390/pr12102128/s1>, Figure S1. Chemical structure of Rhodamine B (RhB). Table S1. Tap water composition. Figure S2. RhB calibration curve; Figure S3. ROTOCAV (E-PIC S.r.l., Italy) rotor-stator device; Figure S4. Hybrid HC/ED plasma reactor; Figure S5. Pseudo first-order linearization of experimental data of lab-scale US-assisted degradation treatments; Figure S6. Ozone bubbling into the RhB solution; Figure S7. Ct/Co dimensionless profile of treatment carried out inside the hybrid HC/ED plasma reactor by switching off the ED (HC alone); Figure S8. Pseudo first-order linearization of experimental data of HC/ED plasma-assisted degradation treatments. Figure S9. UV-vis spectra of HC/ED plasma-assisted degradation treatments carried out with an inlet pressure of (a) 10 bar, (b) 15 bar, and (c) 20 bar.

Author Contributions: Conceptualization, F.V., A.V.K. and E.C.G.; methodology, F.V., D.C., A.V.K., V.B. and E.C.G.; formal analysis, F.V. and E.C.G.; investigation, F.V.; data curation, E.C.G., A.V.K. and G.C.; writing—original draft preparation, F.V.; writing—review and editing, E.C.G.; supervision, E.C.G. and G. C.; All authors have read and agreed to the published version of the manuscript.

Funding: This research received no external funding.

Data Availability Statement: All the data are available in the supporting material.

Acknowledgments: F.V., E.C.G., and G.C. gratefully acknowledge the University of Turin for the financial support (Ricerca Locale 2024), and A.K. acknowledges the IGIC RAS state funds assignment.

Conflicts of Interest: Authors Daniele Crudo and Valentina Bosco were the funders of the company E-PIC Srl. The remaining authors declare that the research was conducted in the absence of any commercial or financial relationships that could be construed as a potential conflict of interest because several technologies and processes were compared.

Appendix A

Table A1. Degradation rate values of lab-scale US and US/H₂O₂ treatments.

Treatment Time (min)	Degradation Rate (%)		
	US Alone	US/H ₂ O ₂ 1:100 (RhB: H ₂ O ₂)	US/H ₂ O ₂ 1:200 (RhB: H ₂ O ₂)
5	7	6	4
10	12	11	11
20	27	27	28
30	45	44	52
45	60	67	75
60	72	82	90

Table A2. Degradation rate values of pilot-scale rotor-stator HC-assisted degradation treatments.

Treatment Time (min)	Degradation Rate (%)	
	HC Alone	HC/H ₂ O ₂ 1:200 (RhB: H ₂ O ₂)
5	1	2
10	2	5
20	5	11
30	8	17
45	11	25
60	13	33

Table A3. Degradation rate values of HC/ED plasma-assisted degradation treatments in loop configuration.

Treatment Time (min)	Degradation Rate (%)		
	10 bar	15 bar	20 bar
1	40	53	64
2	56	76	84
5	79	93	97
10	94	98	98

References

- Available online: <https://www.europarl.europa.eu/topics/en/article/20201208STO93327/the-impact-of-textile-production-and-waste-on-the-environment-infographics#:~:text=Textile%20production%20is%20estimated%20to,up%20in%20the%20food%20chain> (accessed on 1 July 2024).
- Velusamy, S.; Roy, A.; Sundaram, S.; Kumar Mallick, T. A review on heavy metal ions and containing dyes removal through graphene oxide-based adsorption strategies for textile wastewater treatment. *Chem. Rec.* **2021**, *21*, 1570–1610. [[CrossRef](#)]
- Mohod, A.V.; Momotko, M.; Shah, N.S.; Marchel, M.; Imran, M.; Kong, L.; Boczkaj, G. Degradation of Rhodamine dyes by Advanced Oxidation Processes (AOPs)–Focus on cavitation and photocatalysis–A critical review. *Water Resour. Ind.* **2023**, *30*, 100220. [[CrossRef](#)]
- Al-Tameemi, M.N.A. Detection of gain enhancement in laser-induced fluorescence of rhodamine B lasing dye by silicon dioxide nanostructures-coated cavity. *Photonic Sens.* **2018**, *8*, 80–87. [[CrossRef](#)]
- Deng, F.; Xu, Z. Heteroatom-substituted rhodamine dyes: Structure and spectroscopic properties. *Zhongguo Hua Xue Kuai Bao Chin. Chem. Lett.* **2019**, *30*, 1667–1681. [[CrossRef](#)]
- Kolmakov, K.; Belov, V.N.; Bierwagen, J.; Ringemann, C.; Müller, V.; Eggeling, C.; Hell, S.W. Red-emitting rhodamine dyes for fluorescence microscopy and nanoscopy. *Chemistry* **2010**, *16*, 158–166. [[CrossRef](#)]
- Ugwu, M.C.; Oli, A.; Esimone, C.O.; Agu, R.U. Organic cation rhodamines for screening organic cation transporters in early stages of drug development. *J. Pharmacol. Toxicol. Methods* **2016**, *82*, 9–19. [[CrossRef](#)]
- Elbakry, S.; Ali, M.E.A.; Abouelfadl, M.; Badway, N.A.; Salam, K.M.M. Effective removal of organic compounds using a novel cellulose acetate coated by PA/g-CN/Ag nanocomposite membranes. *Surf. Interfaces* **2022**, *29*, 101748. [[CrossRef](#)]
- Li, C.-X.; Wang, R.; Sun, W.; Cui, K.; Fu, X.Z.; Cui, M.; Liu, Y. Efficient degradation of Rhodamine B by visible-light-driven biomimetic Fe(III) complex/peroxymonosulfate system: The key role of FeV=O. *J. Environ. Chem. Eng.* **2024**, *12*, 113288. [[CrossRef](#)]
- Anis, S.F.; Hashaikeh, R.; Hilal, N. Microfiltration membrane processes: A review of research trends over the past decade. *J. Water Process Eng.* **2019**, *32*, 100941. [[CrossRef](#)]
- Vedenyapina, M.D.; Kurmysheva, A.Y.; Rakishev, A.K.; Kryazhev, Y.G. Activated carbon as sorbents for treatment of pharmaceutical wastewater. *Solid Fuel Chem.* **2019**, *53*, 382–394. [[CrossRef](#)]
- Shen, K.; Gondal, M.A. Removal of hazardous Rhodamine dye from water by adsorption onto exhausted coffee ground. *J. Saudi Chem. Soc.* **2017**, *21*, S120–S127. [[CrossRef](#)]
- Kidak, R.; Ince, N.H. Ultrasonic destruction of phenol and substituted phenols: A review of current research. *Ultrason. Sonochem.* **2006**, *13*, 195–199. [[CrossRef](#)]
- Vinayagam, V.; Palani, K.N.; Ganesh, S.; Rajesh, S.; Akula, V.V.; Avoodaiappan, R.; Pugazhendhi, A. Recent developments on advanced oxidation processes for degradation of pollutants from wastewater with focus on antibiotics and organic dyes. *Environ. Res.* **2024**, *240*, 117500. [[CrossRef](#)] [[PubMed](#)]
- Liu, P.; Wu, Z.; Cannizzo, F.T.; Mantegna, S.; Cravotto, G. Removal of antibiotics from milk via ozonation in a vortex reactor. *J. Hazard. Mater.* **2022**, *440*, 129642. [[CrossRef](#)]
- Verdini, F.; Calcio Gaudino, E.; Canova, E.; Colia, M.C.; Cravotto, G. Highly efficient tetracycline degradation under simultaneous hydrodynamic cavitation and electrical discharge plasma in flow. *Ind. Eng. Chem. Res.* **2023**, *62*, 19311–19322. [[CrossRef](#)]
- Semblante, G.U.; Hai, F.I.; Dionysiou, D.D.; Fukushi, K.; Price, W.E.; Nghiem, L.D. Holistic sludge management through ozonation: A critical review. *J. Environ. Manag.* **2017**, *185*, 79–95. [[CrossRef](#)]
- Rekhate, C.V.; Srivastava, J.K. Recent advances in ozone-based advanced oxidation processes for treatment of wastewater–A review. *Chem. Eng. J. Adv.* **2020**, *3*, 100031. [[CrossRef](#)]
- Chandrasekara Pillai, K.; Kwon, T.O.; Moon, I.S. Degradation of wastewater from terephthalic acid manufacturing process by ozonation catalyzed with Fe²⁺, H₂O₂ and UV light: Direct versus indirect ozonation reactions. *Appl. Catal. B Environ.* **2009**, *91*, 319–328. [[CrossRef](#)]
- Mecha, A.C.; Onyango, M.S.; Ochieng, A.; Momba, M.N.B. Impact of ozonation in removing organic micro-pollutants in primary and secondary municipal wastewater: Effect of process parameters. *Water Sci. Technol.* **2016**, *74*, 756–765. [[CrossRef](#)] [[PubMed](#)]
- Mecha, A.C.; Chollom, M.N. Photocatalytic ozonation of wastewater: A review. *Environ. Chem. Lett.* **2020**, *18*, 1491–1507. [[CrossRef](#)]

22. Saxena, S.; Saharan, V.K.; George, S. Enhanced synergistic degradation efficiency using hybrid hydrodynamic cavitation for treatment of tannery waste effluent. *J. Clean. Prod.* **2018**, *198*, 1406–1421. [[CrossRef](#)]
23. Chiang, Y.P.; Liang, Y.Y.; Chang, C.N.; Chao, A.C. Differentiating ozone direct and indirect reactions on decomposition of humic substances. *Chemosphere* **2006**, *65*, 2395–2400. [[CrossRef](#)]
24. Chu, W.; Ching, M.H. Modeling the ozonation of 2,4-dichlorophoxyacetic acid through a kinetic approach. *Water Res.* **2003**, *37*, 39–46. [[CrossRef](#)]
25. Cuiping, B.; Xianfeng, X.; Wenqi, G.; Dexin, F.; Mo, X.; Zhongxue, G.; Nian, X. Removal of rhodamine B by ozone-based advanced oxidation process. *Desalination* **2011**, *278*, 84–90. [[CrossRef](#)]
26. Zawadzki, P.; Deska, M. Degradation efficiency and kinetics analysis of an advanced oxidation process utilizing ozone, hydrogen peroxide and persulfate to degrade the dye rhodamine B. *Catalysts* **2021**, *11*, 974. [[CrossRef](#)]
27. Zajda, M.; Aleksander-Kwaterczak, U. Wastewater treatment methods for effluents from the confectionery industry—an overview. *J. Ecol. Eng.* **2019**, *20*, 293–304. [[CrossRef](#)]
28. Lops, C.; Ancona, A.; Di Cesare, K.; Dumontel, B.; Garino, N.; Canavese, G.; Cauda, V. Sonophotocatalytic degradation mechanisms of Rhodamine B dye via radicals generation by micro- and nano-particles of ZnO. *Appl. Catal. B Environ.* **2019**, *243*, 629–640. [[CrossRef](#)]
29. Paździor, K.; Bilińska, L.; Ledakowicz, S. A review of the existing and emerging technologies in the combination of AOPs and biological processes in industrial textile wastewater treatment. *Chem. Eng. J.* **2019**, *376*, 120597. [[CrossRef](#)]
30. Movahed, S.M.A.; Calgaro, L.; Marcomini, A. Trends and characteristics of employing cavitation technology for water and wastewater treatment with a focus on hydrodynamic and ultrasonic cavitation over the past two decades: A Scientometric analysis. *Sci. Total Environ.* **2023**, *858*, 159802. [[CrossRef](#)]
31. Manson, T.J. *Practical Sonochemistry: User's Guide in Chemistry and Chemical Engineering*; Ellis Horwood Ltd.: Chichester, UK, 1992.
32. Gogate, P.R. Application of cavitation reactors for water disinfection: Current status and path forward. *J. Environ. Manag.* **2007**, *85*, 801–815. [[CrossRef](#)] [[PubMed](#)]
33. Kentish, S.; Ashokkumar, M. The physical and chemical effects of ultrasound. In *Ultrasound Technologies for Food and Bioprocessing*; Food Engineering Series; Feng, H., Barbosa-Canovas, G., Weiss, J., Eds.; Springer: New York, NY, USA, 2011; pp. 1–12. [[CrossRef](#)]
34. Mason, T.J.; Copley, A.J.; Graves, J.E.; Morgan, D. New evidence for the inverse dependence of mechanical and chemical effects on the frequency of ultrasound. *Ultrason. Sonochem.* **2011**, *18*, 226–230. [[CrossRef](#)] [[PubMed](#)]
35. Mason, T.J.; Lorimer, J.P.; Bates, D.M.; Zhao, Y. Dosimetry in sonochemistry: The use of aqueous terephthalate ion as a fluorescence monitor. *Ultrason. Sonochem.* **1994**, *1*, 91–95. [[CrossRef](#)]
36. Lim, M.; Son, Y.; Khim, J. The effects of hydrogen peroxide on the sonochemical degradation of phenol and bisphenol A. *Ultrason. Sonochem.* **2014**, *21*, 1976–1981. [[CrossRef](#)] [[PubMed](#)]
37. Calcio Gaudino, E.; Grillo, G.; Tabasso, S.; Stevanato, L.; Cravotto, G.; Marjamaa, K.; Schories, G. Optimization of ultrasound pretreatment and enzymatic hydrolysis of wheat straw: From lab to semi-industrial scale. *J. Clean. Prod.* **2022**, *380*, 134897. [[CrossRef](#)]
38. Xu, D.; Ma, H. Degradation of rhodamine B in water by ultrasound-assisted TiO₂ photocatalysis. *J. Clean. Prod.* **2021**, *313*, 127758. [[CrossRef](#)]
39. Ye, Y.F.; Zhu, Y.; Lu, N.; Wang, X.; Su, Z. Treatment of rhodamine B with cavitation technology: Comparison of hydrodynamic cavitation with ultrasonic cavitation. *RSC Adv.* **2021**, *11*, 5096–5106. [[CrossRef](#)] [[PubMed](#)]
40. Mehrdad, A.; Hashemzadeh, R. Ultrasonic degradation of Rhodamine B in the presence of hydrogen peroxide and some metal oxide. *Ultrason. Sonochem.* **2010**, *17*, 168–172. [[CrossRef](#)]
41. Badve, M.; Gogate, P.; Pandit, A.; Csoka, L. Hydrodynamic cavitation as a novel approach for wastewater treatment in wood finishing industry. *Sep. Purif. Technol.* **2013**, *106*, 15–21. [[CrossRef](#)]
42. Zheng, H.; Zheng, Y.; Zhu, J. Recent developments in hydrodynamic cavitation reactors: Cavitation mechanism, reactor design, and applications. *Engineering* **2022**, *19*, 180–198. [[CrossRef](#)]
43. Ferrari, A. Fluid dynamics of acoustic and hydrodynamic cavitation in hydraulic power systems. *Proc. R. Soc. A: Math. Phys. Eng. Sci.* **2017**, *473*, 20160345. [[CrossRef](#)]
44. Sun, X.; Chen, S.; Liu, J.; Zhao, S.; Yoon, J.Y. Hydrodynamic cavitation: A promising technology for industrial-scale synthesis of nanomaterials. *Front. Chem.* **2020**, *8*, 259. [[CrossRef](#)] [[PubMed](#)]
45. Darandale, G.R.; Jadhav, M.V.; Warade, A.R.; Hakke, V.S. Hydrodynamic cavitation a novel approach in wastewater treatment: A review. *Mater. Today Proc.* **2023**, *77*, 960–968. [[CrossRef](#)]
46. Wang, B.; Su, H.; Zhang, B. Hydrodynamic cavitation as a promising route for wastewater treatment—A review. *Chem. Eng. J.* **2021**, *412*, 128685. [[CrossRef](#)]
47. Khajeh, M.; Taheri, E.; Amin, M.M.; Fatehizadeh, A.; Bedia, J. Combination of hydrodynamic cavitation with oxidants for efficient treatment of synthetic and real textile wastewater. *J. Water Process Eng.* **2022**, *49*, 103143. [[CrossRef](#)]
48. Available online: <https://www.fbcitalia.it/blog/costo-energia-elettrica-al-kwh-per-aziende-quanto-e-importante> (accessed on 1 July 2024).
49. Available online: <https://www.epic-srl.com/it/sistemi-cavitazionali/pretrattamento-biomasse> (accessed on 1 July 2024).
50. Crudo, D.; Bosco, V.; Cavaglià, G.; Grillo, G.; Mantegna, S.; Cravotto, G. Biodiesel production process intensification using a rotor-stator type generator of hydrodynamic cavitation. *Ultrason. Sonochem.* **2016**, *33*, 220–225. [[CrossRef](#)]

51. Mishra, K.P.; Gogate, P.R. Intensification of degradation of Rhodamine B using hydrodynamic cavitation in the presence of additives. *Sep. Purif. Technol.* **2010**, *75*, 385–391. [[CrossRef](#)]
52. Wang, X.; Wang, J.; Guo, P.; Guo, W.; Wang, C. Degradation of rhodamine B in aqueous solution by using swirling jet-induced cavitation combined with H₂O₂. *J. Hazard. Mater.* **2009**, *169*, 486–491. [[CrossRef](#)]
53. Aggelopoulos, C.A. Recent advances of cold plasma technology for water and soil remediation: A critical review. *Chem. Eng. J.* **2022**, *428*, 131657. [[CrossRef](#)]
54. Sanito, R.C.; You, S.J.; Wang, Y.F. Degradation of contaminants in plasma technology: An overview. *J. Hazard. Mater.* **2022**, *424*, 127390. [[CrossRef](#)]
55. Murugesan, P.; Monica, E.; Moses, J.A.; Anandharamkrishnan, C. Water decontamination using non-thermal plasma: Concepts, applications, and prospects. *Environ. Chem. Eng.* **2020**, *8*, 104377. [[CrossRef](#)]
56. Jiang, B.; Zheng, J.; Qiu, S.; Wu, M.; Zhang, Q.; Yan, Z.; Xue, Q. Review on electrical discharge plasma technology for wastewater remediation. *Chem. Eng. J.* **2014**, *236*, 348–368. [[CrossRef](#)]
57. Kyere-Yeboah, K.; Bique, I.K.; Qiao, X.C. Advances of non-thermal plasma discharge technology in degrading recalcitrant wastewater pollutants. A comprehensive review. *Chemosphere* **2023**, *320*, 138061. [[CrossRef](#)] [[PubMed](#)]
58. Abramov, V.O.; Abramova, A.V.; Cravotto, G.; Nikonov, R.V.; Fedulov, I.S.; Ivanov, V.K. Flow-mode water treatment under simultaneous hydrodynamic cavitation and plasma. *Ultrason. Sonochem.* **2021**, *70*, 105323. [[CrossRef](#)]
59. Pereira, T.C.; Flores, E.M.M.; Abramova, A.V.; Verdini, F.; Calcio Gaudino, E.; Bucciol, F.; Cravotto, G. Simultaneous hydrodynamic cavitation and glow plasma discharge for the degradation of metronidazole in drinking water. *Ultrason. Sonochem.* **2023**, *95*, 106388. [[CrossRef](#)] [[PubMed](#)]
60. Verdini, F.; Abramova, A.; Boffa, L.; Calcio Gaudino, E.; Cravotto, G. The unveiling of a dynamic duo: Hydrodynamic cavitation and cold plasma for the degradation of furosemide in wastewater. *Sci. Rep.* **2024**, *14*, 6805. [[CrossRef](#)]
61. Verdini, F.; Canova, E.; Solarino, R.; Calcio Gaudino, E.; Cravotto, G. Integrated physicochemical processes to tackle high-COD wastewater from pharmaceutical industry. *Environ. Pollut.* **2024**, *342*, 123041. [[CrossRef](#)]
62. Nie, S.; Qin, T.; Ji, H.; Nie, S.; Dai, Z. Synergistic effect of hydrodynamic cavitation and plasma oxidation for the degradation of Rhodamine B dye wastewater. *J. Water Proc. Eng.* **2022**, *49*, 103022. [[CrossRef](#)]
63. Komarov, S.; Yamamoto, T.; Fang, Y.; Hariu, D. Combined effect of acoustic cavitation and pulsed discharge plasma on wastewater treatment efficiency in a circulating reactor: A case study of Rhodamine B. *Ultrason. Sonochem.* **2020**, *68*, 105236. [[CrossRef](#)]
64. Xu, Y.; Komarov, S.; Yamamoto, T.; Kutsuzawa, T. Enhancement and mechanism of rhodamine B decomposition in cavitation-assisted plasma treatment combined with Fenton reactions. *Catalysts* **2022**, *12*, 1491. [[CrossRef](#)]

Disclaimer/Publisher's Note: The statements, opinions and data contained in all publications are solely those of the individual author(s) and contributor(s) and not of MDPI and/or the editor(s). MDPI and/or the editor(s) disclaim responsibility for any injury to people or property resulting from any ideas, methods, instructions or products referred to in the content.